PROCEEDINGS OF SCIENCE

Lattice QCD calculations of nucleon transverse momentum-dependent parton distributions (TMDs) at 170 MeV pion mass

M. Engelhardt[*a†], **B. Musch**[b], **T. Bhattacharya**[c], **R. Gupta**[c], **P. Hägler**[b], **S. Krieg**[d,e], **J. Negele**[f], **A. Pochinsky**[f], **S. Syritsyn**[g] **and B. Yoon**[c]

[a] *Department of Physics, New Mexico State University, Las Cruces, NM 88003, USA*
[b] *Institut für Theoretische Physik, Universität Regensburg, 93040 Regensburg, Germany*
[c] *Theoretical Division, Los Alamos National Laboratory, Los Alamos, NM 87545, USA*
[d] *Bergische Universität Wuppertal, 42119 Wuppertal, Germany*
[e] *IAS, Jülich Supercomputing Centre, Forschungszentrum Jülich, 52425 Jülich, Germany*
[f] *Center for Theoretical Physics, Massachusetts Institute of Technology, Cambridge, MA 02139, USA*
[g] *Theory Center, Thomas Jefferson National Accelerator Facility, Newport News, VA 23606, USA*
[†] *E-mail:* engel@nmsu.edu

An exploration of nucleon TMD observables at a substantially lower pion mass, 170 MeV, than used in previous lattice TMD calculations is presented. On a corresponding RBC/UKQCD domain wall fermion ensemble, TMDs are extracted from nucleon matrix elements of a bilocal quark operator containing a staple-shaped gauge link. Appropriate TMD ratios are constructed to cancel divergences associated with the gauge link. In particular, results associated with the time-reversal odd Sivers effect and with the quark transversity are reported. They are compared with previous domain wall fermion calculations at 297 MeV pion mass with a view to exploring whether these observables vary strongly as a function of pion mass in the chiral regime.

The 33rd International Symposium on Lattice Field Theory
14 - 18 July 2015
Kobe International Conference Center, Kobe, Japan

[*] Speaker.

PoS(LATTICE 2015)117

1. Introduction

In the description of hadron structure, transverse momentum-dependent parton distribution functions [1] (TMDs) play a role complementary to generalized parton distributions (GPDs). Whereas GPDs encode information about the transverse spatial distribution of partons (through Fourier transformation with respect to the momentum transfer), TMDs contain information about the transverse momentum distribution of partons. Cast in a Lorentz frame in which the hadron of mass m_h propagates with a large momentum in the 3-direction, $P^+ \equiv (P^0 + P^3)/\sqrt{2} \gg m_h$, the quark momentum components scale such that TMDs are principally functions $f(x, k_T)$ of the quark longitudinal momentum fraction $x = k^+/P^+$ and the quark transverse momentum vector k_T, with the dependence on the component $k^- \equiv (k^0 - k^3)/\sqrt{2} \ll m_h$ becoming ignorable in this limit. The function $f(x, k_T)$ will thus be regarded as having been integrated over k^-.

Experimentally, TMDs manifest themselves in angular asymmetries observed in processes such as semi-inclusive deep inelastic scattering (SIDIS) and the Drell-Yan (DY) process. Corresponding signatures have emerged at COMPASS, HERMES and JLab [2–4], and that has motivated targeting a significant part of the physics program at future experiments in this direction, e.g., at the upgraded JLab 12 GeV facility and at the proposed electron-ion collider (EIC). Relating the experimental signature to the hadron structure encoded in TMDs requires a suitable factorization framework, the one having been advanced in [5–8] being particularly well-suited for connecting phenomenology to lattice QCD. Factorization in the TMD context is considerably more involved than standard collinear factorization, with the resulting TMDs in general being process-dependent, via initial and/or final state interactions between the struck quark and the hadron remnant.

2. Definition of TMD observables

The definition of TMD observables amenable to lattice evaluation has been laid out in detail in [9]. Summarizing briefly, the starting point is the fundamental correlator

$$\widetilde{\Phi}^{[\Gamma]}_{\text{unsubtr.}}(b, P, S, \ldots) \equiv \frac{1}{2} \langle P,S| \, \bar{q}(0) \, \Gamma \, \mathscr{U}[0, \eta v, \eta v + b, b] \, q(b) \, |P,S\rangle \tag{2.1}$$

where S denotes the spin of the hadron and Γ stands for an arbitrary γ-matrix structure. The staple-shaped gauge connection $\mathscr{U}$ follows straight-line paths connecting the positions given in its argument; the unit vector v thus specifies the direction of the staple, whereas η parametrizes its length. The presence of $\mathscr{U}$ introduces divergences in $\widetilde{\Phi}^{[\Gamma]}_{\text{unsubtr.}}$ additional to the wave function renormalizations of the quark operators; these divergences accordingly must ultimately be compensated by additional "soft factors", which are expected to be multiplicative and do not need to be specified in detail here, since only appropriate ratios in which they then presumably cancel will ultimately be considered. In order to regularize rapidity divergences, the staple direction v is taken slightly off the light cone into the space-like region [5, 6], with perturbative evolution equations governing the approach to the light cone [7]. A useful parameter characterizing how close v is to the light cone is the Collins-Soper evolution parameter $\hat{\zeta} = v \cdot P/(|v|\,|P|)$, in terms of which the light cone is approached for $\hat{\zeta} \to \infty$.

The correlator (2.1) can be decomposed in terms of invariant amplitudes $\widetilde{A}_{iB}$. Listing only the components relevant for the Sivers effect and the transversity discussed in detail below,

$$\frac{1}{2P^+}\widetilde{\Phi}^{[\gamma^+]}_{\text{unsubtr.}} = \widetilde{A}_{2B} + im_h\varepsilon_{ij}b_iS_j\widetilde{A}_{12B} \tag{2.2}$$

$$\frac{1}{2P^+}\widetilde{\Phi}^{[i\sigma^{i+}\gamma^5]}_{\text{unsubtr.}} = im_h\varepsilon_{ij}b_j\widetilde{A}_{4B} - S_i\widetilde{A}_{9B} - im_h\Lambda b_i\widetilde{A}_{10B} + m_h[(b\cdot P)\Lambda - m_h(b_T\cdot S_T)]b_i\widetilde{A}_{11B}\,, \tag{2.3}$$

where Λ denotes the hadron helicity (i.e., $S^+ = \Lambda P^+/m_h$, $S^- = -\Lambda m_h/2P^+$). These amplitudes are useful in that they can be evaluated in any desired Lorentz frame, including a frame that is particularly suited for the lattice calculation. Specializing to TMDs integrated over momentum fraction x, by considering specifically $b\cdot P = 0$, they serve to define the "generalized Sivers shift"

$$\langle k_y\rangle_{TU}(b_T^2,\ldots) = -m_h\widetilde{A}_{12B}(-b_T^2,\ldots)/\widetilde{A}_{2B}(-b_T^2,\ldots) = m_h\tilde{f}_{1T}^{\perp[1](1)}(b_T^2,\ldots)/\tilde{f}_1^{[1](0)}(b_T^2,\ldots) \tag{2.4}$$

where the right-hand expression introduces the notation in terms of Fourier-transformed TMD moments, for details, cf. [9]. In the $b_T \to 0$ limit, (2.4) formally represents the average transverse momentum k_y of unpolarized ("U") quarks orthogonal to the transverse ("T") spin of the hadron, normalized to the corresponding number of valence quarks. Similarly, one can introduce a generalized tensor charge via the ratio of Fourier-transformed moments of the transversity and unpolarized TMDs,

$$\tilde{h}_1^{[1](0)}(b_T^2,\ldots)/\tilde{f}_1^{[1](0)}(b_T^2,\ldots) = -[\widetilde{A}_{9B}(-b_T^2,\ldots) - m_h^2b^2\widetilde{A}_{11B}(-b_T^2,\ldots)/2]/\widetilde{A}_{2B}(-b_T^2,\ldots)\,. \tag{2.5}$$

In the $b_T \to 0$ limit, this formally reduces to the tensor charge, normalized to the corresponding number of valence quarks. The ratios (2.4) and (2.5) are designed to cancel both multiplicative soft factors associated with the gauge connection $\mathscr{U}$ as well as wave function renormalizations attached to the quark operators in (2.1) at finite physical separation b.

3. Lattice evaluation and results

To access observables such as (2.4) and (2.5) within lattice QCD, one calculates hadron matrix elements of the type (2.1) and then decomposes them into invariant amplitudes, as given in (2.2) and (2.3). For this to be possible, it is crucial to work in a scheme where the four-vectors b and v are generically space-like, for the following reason: By employing a Euclidean time coordinate to project out hadron ground states via Euclidean time evolution, lattice QCD cannot straightforwardly accomodate operators containing Minkowski time separations. The operator of which one takes matrix elements thus has to be defined at a single time. Only if both b and v are space-like is there no obstacle to boosting the problem to a Lorentz frame in which b and v are purely spatial, and evaluating $\widetilde{\Phi}^{[\Gamma]}_{\text{unsubtr.}}$ in that frame. The results extracted for the invariant amplitudes $\widetilde{A}_{iB}$ are then immediately valid also in the original frame in which (2.1) was initially defined, thus completing the determination of quantities of the type (2.4) and (2.5).

Since, in a numerical lattice calculation, the staple extent η necessarily remains finite, two extrapolations must be performed from the generated data, namely, the one to infinite staple length, $\eta \to \infty$, and the extrapolation of the staple direction towards the light cone, $\hat{\zeta} \to \infty$. Whereas the former extrapolation is under control for a range of parameters used in this work, the latter presents

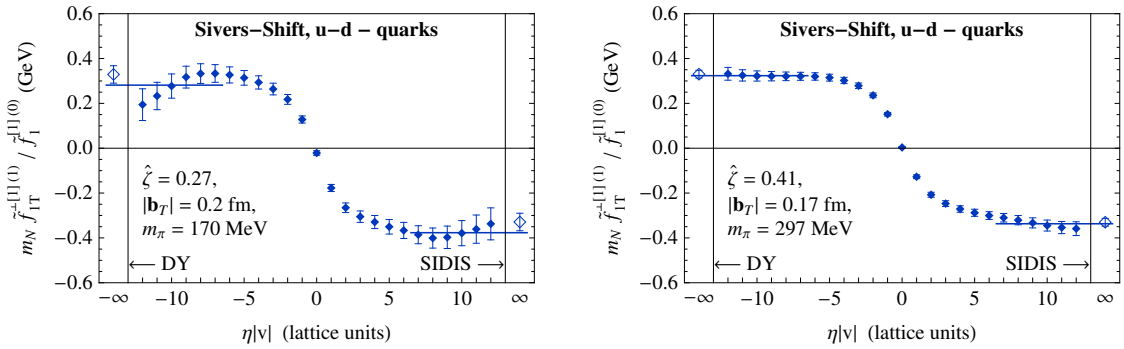

Figure 1: Dependence of the generalized Sivers shift on the staple extent at a fixed b_T and $\hat{\zeta}$, in domain wall fermion calculations at $m_\pi = 170\,\text{MeV}$ (left) and $m_\pi = 297\,\text{MeV}$ (right) [11]. Note that the two panels available for this comparison match fairly well in b_T, but differ somewhat in $\hat{\zeta}$; however, as evidenced by Fig. 3 (right) below, the generalized Sivers shift at $m_\pi = 297\,\text{MeV}$ does not vary significantly in the $\hat{\zeta}$ range in question.

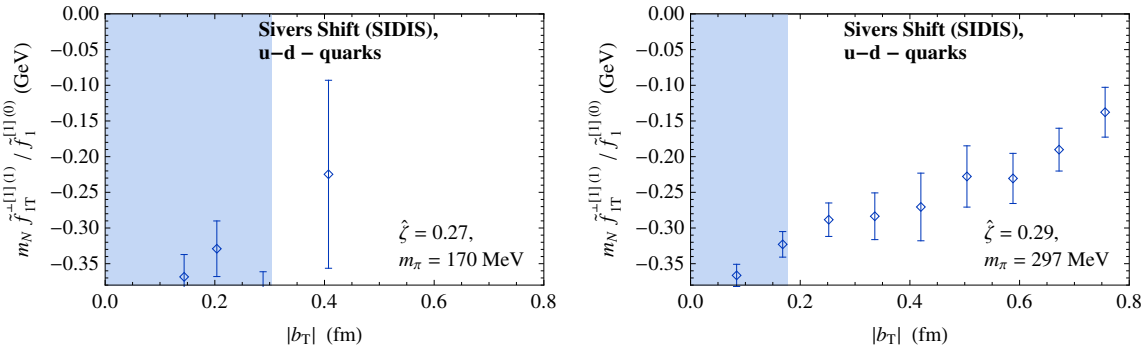

Figure 2: Generalized Sivers shift as a function of b_T in the $\eta \to \infty$ SIDIS limit, at a fixed $\hat{\zeta}$, in domain wall fermion calculations at $m_\pi = 170\,\text{MeV}$ (left) and $m_\pi = 297\,\text{MeV}$ (right) [11].

a challenge, owing to the limited set of hadron momenta P accessible with sufficient statistical accuracy. This issue has been investigated in detail in [10]. The present study focuses instead on another aspect, namely, whether TMD ratios of the type (2.4) and (2.5) display significant variation with the pion mass in the chiral regime. Figs. 1-6 present new data for the isovector[1] generalized Sivers shift (2.4) and generalized tensor charge (2.5) in the nucleon, obtained using an RBC/UKQCD 2+1-flavor domain wall fermion ensemble with a lattice spacing of $a = 0.144\,\text{fm}$, corresponding to a pion mass of $m_\pi = 170\,\text{MeV}$. They are juxtaposed in Figs. 1-6 with corresponding data previously obtained [11] using an RBC/UKQCD 2+1-flavor domain wall fermion ensemble with a lattice spacing of $a = 0.084\,\text{fm}$, corresponding to a pion mass of $m_\pi = 297\,\text{MeV}$. The $m_\pi = 170\,\text{MeV}$ calculation employed 8 source-sink pairs on each of 310 lattices, i.e., 2480 samples, for each matrix element; the $m_\pi = 297\,\text{MeV}$ calculation 8 source-sink pairs on 533 lattices, i.e., 4264 samples.

Fig. 1 displays the dependence of the generalized Sivers shift (2.4) on the staple extent for a given quark separation b_T and a given staple direction characterized by $\hat{\zeta}$. The T-odd behavior of

[1] In the isovector, $u-d$ quark combination, diagrams with operator insertions in disconnected quark loops, which have not been evaluated, cancel.

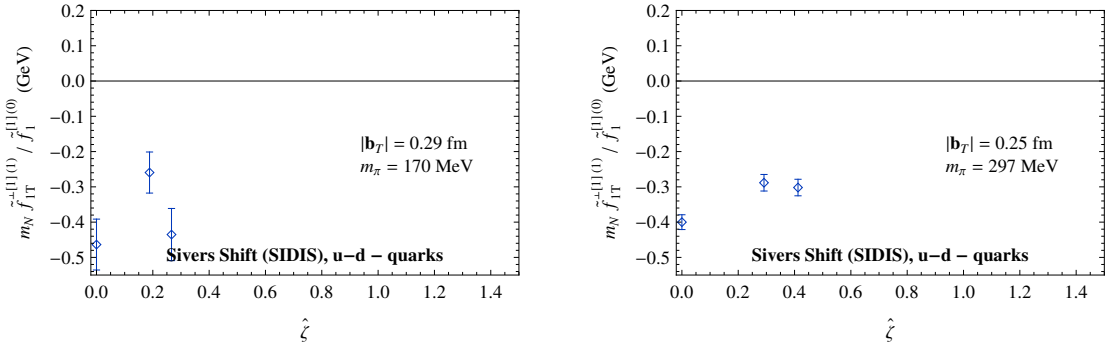

Figure 3: Generalized Sivers shift as a function of $\hat{\zeta}$ in the $\eta \to \infty$ SIDIS limit, at a fixed b_T, in domain wall fermion calculations at $m_\pi = 170\,\mathrm{MeV}$ (left) and $m_\pi = 297\,\mathrm{MeV}$ (right) [11].

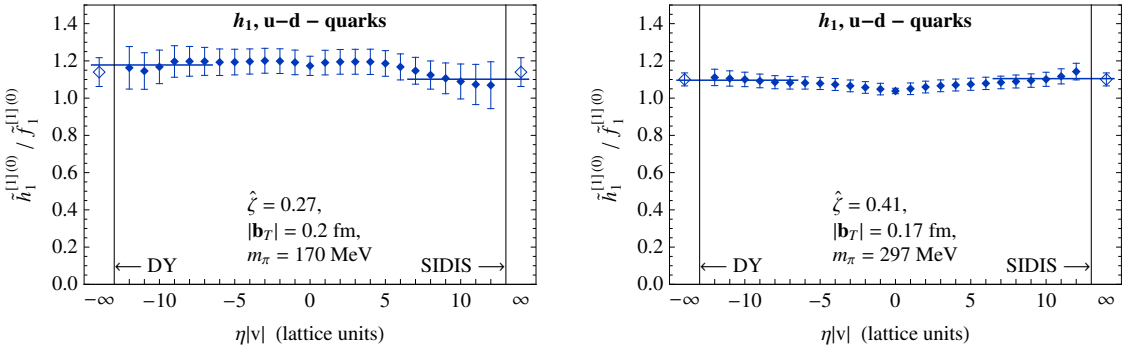

Figure 4: Dependence of the generalized tensor charge on the staple extent at a fixed b_T and $\hat{\zeta}$, in domain wall fermion calculations at $m_\pi = 170\,\mathrm{MeV}$ (left) and $m_\pi = 297\,\mathrm{MeV}$ (right) [11]. Note that, as in Fig. 1, the juxtaposition employs somewhat differing $\hat{\zeta}$ values; however, the variation of the generalized tensor charge with $\hat{\zeta}$ in the range in question is not significant, cf. Fig. 6.

this observable is evident, with $\eta \to \infty$ corresponding to the SIDIS limit, and $\eta \to -\infty$ yielding the DY limit. The data level off to approach identifiable plateaux as the staple length grows, with the lighter pion mass data being affected by considerably stronger statistical fluctuations. The limiting SIDIS and DY values, represented by the open symbols, are extracted by imposing antisymmetry in η, allowing one to appropriately average the $\eta \to \pm\infty$ plateau values. Fig. 2 summarizes the results in the SIDIS limit for different b_T at a given $\hat{\zeta}$, where the shaded area below $|b_T| = 2a$ indicates the region where the results may be significantly affected by finite lattice cutoff effects. The strong statistical fluctuations in the $m_\pi = 170\,\mathrm{MeV}$ ensemble manifest themselves in what appears to be an outlier at $|b_T| = 0.29\,\mathrm{fm}$; only a tenuous signal is obtained for the generalized Sivers shift in the region $|b_T| > 2a$. Fig. 3 in turn summarizes the dependence of the generalized Sivers shift on the Collins-Soper evolution parameter $\hat{\zeta}$, with $|b_T|$ kept fixed. The same outlier as seen in Fig. 2 (left) is again present, at $\hat{\zeta} = 0.27$. Only a very limited range of $\hat{\zeta}$ was accessible, corresponding to the limited set of nucleon momenta P available; no clear large $\hat{\zeta}$ trend can be identified from the data obtained within the present study. Note, however, that a dedicated calculation can indeed provide information about the large $\hat{\zeta}$ limit in favorable circumstances [10]. Figs. 2 and 3 suggest

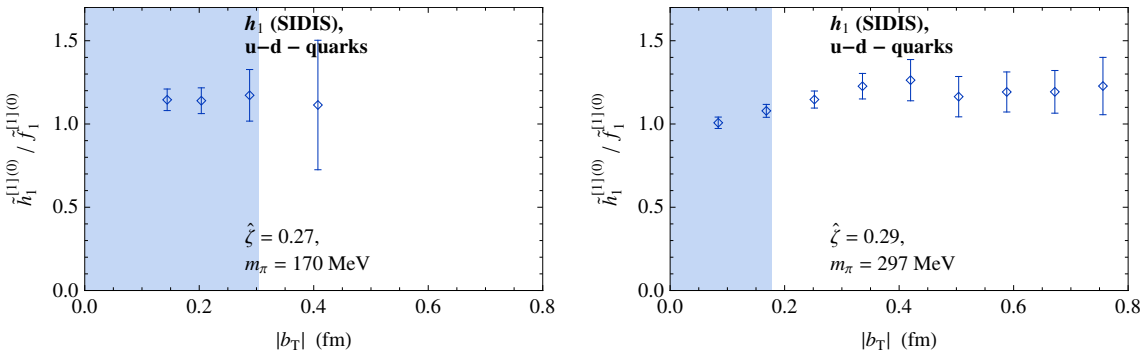

Figure 5: Generalized tensor charge as a function of b_T in the $\eta \to \infty$ SIDIS limit, at a fixed $\hat{\zeta}$, in domain wall fermion calculations at $m_\pi = 170\,\mathrm{MeV}$ (left) and $m_\pi = 297\,\mathrm{MeV}$ (right) [11].

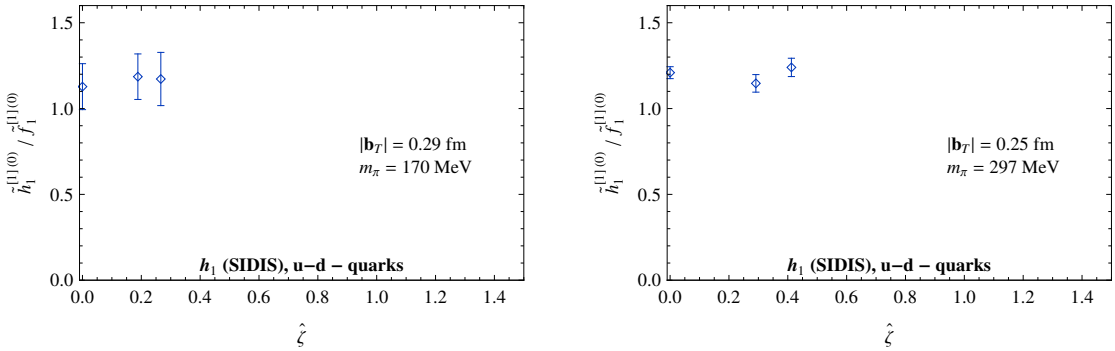

Figure 6: Generalized tensor charge as a function of $\hat{\zeta}$ in the $\eta \to \infty$ SIDIS limit, at a fixed b_T, in domain wall fermion calculations at $m_\pi = 170\,\mathrm{MeV}$ (left) and $m_\pi = 297\,\mathrm{MeV}$ (right) [11].

that, within the large uncertainties affecting the $m_\pi = 170\,\mathrm{MeV}$ calculation, the data at the two pion masses are compatible. However, more accurate calculations at low pion masses will be necessary to draw substantive conclusions about the m_π-dependence of the generalized Sivers shift.

A somewhat more stable picture regarding statistical fluctuations is afforded by the generalized tensor charge (2.5). Fig. 4 shows its dependence on the staple extent for a given quark separation b_T and a given staple direction characterized by $\hat{\zeta}$. This is a T-even quantity, with the SIDIS and DY limits coinciding; the asymptotic values represented by the open symbols are obtained by averaging both limits. Fig. 5 summarizes the SIDIS limit data for given $\hat{\zeta}$ as a function of b_T, similar to Fig. 2. A somewhat more stable numerical behavior is observed; again, no significant difference between the results at $m_\pi = 170\,\mathrm{MeV}$ and $m_\pi = 297\,\mathrm{MeV}$ is seen, keeping in mind the sizeable uncertainties of the data at the lighter pion mass. Fig. 6, which conversely displays the dependence of the generalized tensor charge on the Collins-Soper evolution parameter $\hat{\zeta}$, with $|b_T|$ kept fixed, likewise exhibits no significant variation of that observable with m_π.

4. Summary

Within a continuing exploration of TMD calculations using lattice QCD, the principal focus of the present work is whether TMD ratios of the type (2.4) and (2.5) display significant variation

with the pion mass in the chiral regime. To this end, new data for these observables obtained at the pion mass $m_\pi = 170\,\mathrm{MeV}$ were compared with data previously extracted [11] from calculations at $m_\pi = 297\,\mathrm{MeV}$. The results of the calculation at $m_\pi = 170\,\mathrm{MeV}$ display strong statistical fluctuations. For the generalized Sivers shift (2.4), only tenuous signals, with prominent outliers, were obtained once the transverse quark separation $|b_T|$ became appreciable. The generalized tensor charge (2.5) proved to be somewhat more numerically stable, but is still subject to substantial statistical uncertainties. Keeping in mind these large statistical fluctuations, the juxtaposition of the $m_\pi = 170\,\mathrm{MeV}$ and $m_\pi = 297\,\mathrm{MeV}$ data suggests that the TMD ratios (2.4) and (2.5) are fairly stable as a function of pion mass in the chiral regime; no statistically significant variation is seen, within the large uncertainties. However, it is clearly necessary to obtain more accurate, higher statistics data at light pion masses to draw any substantive conclusions about the m_π-dependence of TMD ratios as the physical pion mass is approached.

Acknowledgements

Computations were performed using resources provided by the U.S. DOE Office of Science through the National Energy Research Scientific Computing Center (NERSC), a DOE Office of Science User Facility, under Contract No. DE-AC02-05CH11231, as well as through facilities of the USQCD Collaboration, employing the Chroma software suite [12]. The RBC/UKQCD collaboration is gratefully acknowledged for providing the gauge ensembles analyzed in this work. Support by the Heisenberg-Fellowship program of the DFG (P.H.), SFB/TRR-55 (S.K.), the RIKEN Foreign Postdoctoral Researcher Program (BNL) as well as the Nathan Isgur Fellowship (JLab) (S.S.), and the U.S. DOE and the Office of Nuclear Physics through grants DE-FG02-96ER40965 (M.E.), DE-SC0011090 (J.N.) and DE-FC02-06ER41444 (A.P.) is acknowledged. R.G., T.B. and B.Y. are supported by DOE grant DE-KA-1401020 and the LDRD program at LANL.

References

[1] D. Boer, M. Diehl, R. Milner, R. Venugopalan, W. Vogelsang, *et al.*, `arXiv:1108.1713`.

[2] M. Alekseev, *et al.*, COMPASS Collaboration, *Phys. Lett.* **B673** (2009) 127.

[3] A. Airapetian, *et al.*, HERMES Collaboration, *Phys. Rev. Lett.* **103** (2009) 152002.

[4] H. Avakian, *et al.*, CLAS Collaboration, *Phys. Rev. Lett.* **105** (2010) 262002.

[5] S. M. Aybat and T. C. Rogers, *Phys. Rev.* **D 83** (2011) 114042.

[6] J. C. Collins, *Foundations of Perturbative QCD* (Cambridge University Press, 2011).

[7] S. M. Aybat, J. C. Collins, J.-W. Qiu and T. C. Rogers, *Phys. Rev.* **D 85** (2012) 034043.

[8] J. C. Collins and T. C. Rogers, *Phys. Rev.* **D 87** (2013) 034018.

[9] B. Musch, P. Hägler, M. Engelhardt, J. W. Negele and A. Schäfer, *Phys. Rev.* **D 85** (2012) 094510.

[10] M. Engelhardt, B. Musch, P. Hägler, A. Schäfer and J. W. Negele, *Int. J. Mod. Phys. Conf. Ser.* **37** (2015) 1560034.

[11] M. Engelhardt, B. Musch, T. Bhattacharya, R. Gupta, P. Hägler, J. Negele, A. Pochinsky, A. Schäfer, S. Syritsyn and B. Yoon, *PoS* **LATTICE2014** (2014) 167.

[12] R. G. Edwards and B. Joó, SciDAC Collaboration, *Nucl. Phys. Proc. Suppl.* **140** (2005) 832.